Journal of Magnetic Resonance **138,** 164–166 (1999)
Article ID jmre.1999.1746, available online at http://www.idealibrary.com on IDEAL®

Nuclear Longitudinal Relaxation Time Images by Radiofrequency Field Gradients

F. Humbert, E. Collenne, M. Valtier, and D. Canet[1]

Laboratoire de Méthodologie RMN (UPRESA CNRS 7042; FR CNRS 1742, INCM), Université Henri Poincaré, Nancy I, B.P. 239, 54506 Vandoeuvre-lès-Nancy Cedex, France

Received June 19, 1998; revised December 22, 1998

Combination of the Super Fast Inversion Recovery (SUFIR) method (D. Canet, J. Brondeau, and K. Elbayed, *J. Magn. Reson.* **77, 483 (1988)) and imaging procedures by radiofrequency field gradients (P. Maffei, P. Mutzenhardt, A. Retournard, B. Diter, R. Raulet, J. Brondeau, and D. Canet,** *J. Magn. Reson. A* **107, 40 (1994)) provides spatially resolved maps of longitudinal relaxation times (T_1). In addition to accurate T_1 values, enhanced spatial resolution is obtained.** © 1999 Academic Press

Although most NMR imaging procedures inherently involve some contrast by relaxation times (*1*), quantitation of the latter (i.e., images which exhibit, in the third dimension, the relaxation time values instead of the spin density) is not an easy task. We shall be concerned in this paper with the spatially resolved determination of nuclear longitudinal relaxation times (T_1). Most of the time, T_1 contrast (if desired) is achieved by shortening the repetition rate (between two consecutive scans) in order to enhance regions of short T_1. Obtaining a map (image) of longitudinal relaxation times requires the repetition of the imaging experiment for several values of some interval sensitive to the longitudinal relaxation time (for instance the repetition rate or the recovery period in experiments involving an initial perturbation) and to analyze the evolution curve pertaining to each pixel (*2–7*). Another approach is one-shot in nature as it consists of monitoring the magnetization recovery during a single imaging experiment (*8–10*), according to a strategy early proposed by Look and Locker (*11*).

Some time ago, we devised a method for determining T_1, dubbed Super Fast Inversion Recovery (SUFIR) (*12*), which relies on the comparison of a reference spectrum (S_1 in the following) with a partially relaxed spectrum (S_2 in the following), both experiments being interleaved as shown in Fig. 1 so that the total measuring time is at most twice as large as a conventional "one-pulse" experiment. Choosing the same duration τ for each interval in the sequence (see Fig. 1) allows for a straightforward determination of T_1 together with an accuracy better than 5%, provided that τ lies in the range $0.5\ T_1 - 3\ T_1$ (which is sufficiently broad for most practical applications)

$$T_1 = -\frac{\tau}{\ln(1 - S_2/S_1)}. \qquad [1]$$

It can be emphasized that this procedure amounts to sample in *an optimal way* only two data points of a fast inversion-recovery experiment (*13*). Indeed the final uncertainty on the T_1 value is the lowest one that can be achieved (*14*) due, in particular, to the alternate block acquisition mode which compensates actually for any instrumental drift. Moreover, the

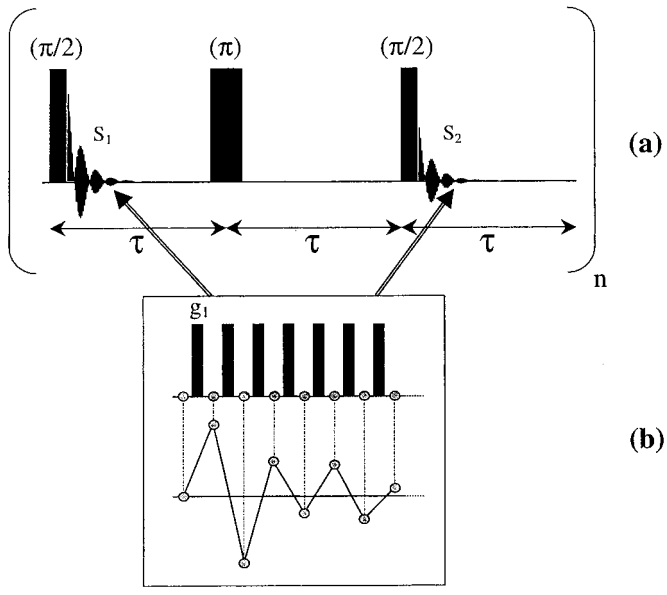

FIG. 1. (a) The basic scheme of the SUFIR experiment which rests on the comparison of a reference spectrum (S_1) with a partially relaxed spectrum (S_2). In order to remove some artifacts the central π pulse is phase cycled according to (x, y, $-x$, $-y$). (b) In the relevant imaging experiment, both acquisitions are replaced by a train of B_1 gradient pulses (g_1) with acquisition of a single data point between two consecutive pulses. The Fourier transform of the pseudo-fid obtained that way yields a spatial profile representative of S_1 or S_2.

[1] To whom correspondence should be addressed. E-mail: dc@meth-rmm.u-nancy.fr.

1090-7807/99 $30.00

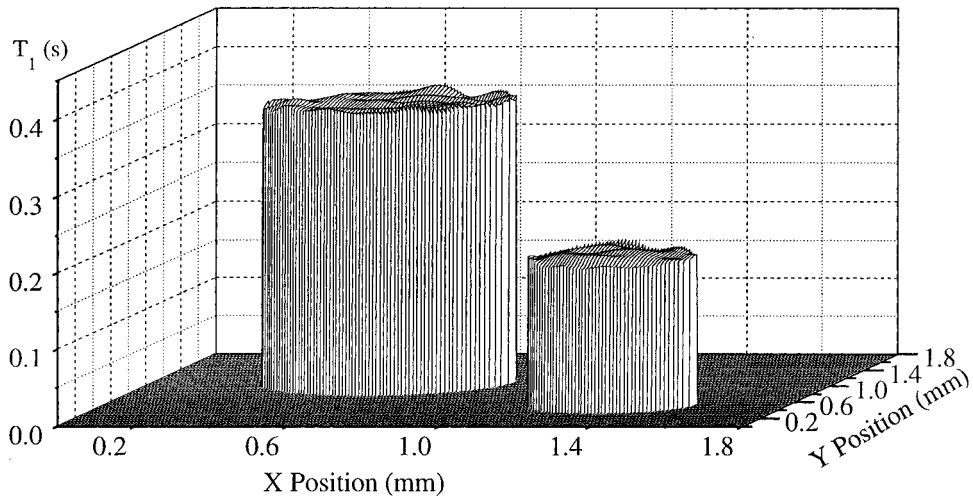

FIG. 2. T_1 map of two capillaries of 785 and 470 μm respective diameters filled with $CuSO_4$ doped water (liquid height: ca. 2 mm). The interval τ of the SUFIR sequence was set to 330 ms and n to 256 (see Fig. 1). Two-dimensional images were obtained by rotating the sample in 3.6° steps; for each rotation the experiment of Fig. 1b was repeated. ^{1}H measurements were performed at 90 MHz with a probe described previously (*18*) delivering a B_1 gradient of 50 G cm^{-1} (sample temperature: 26°C).

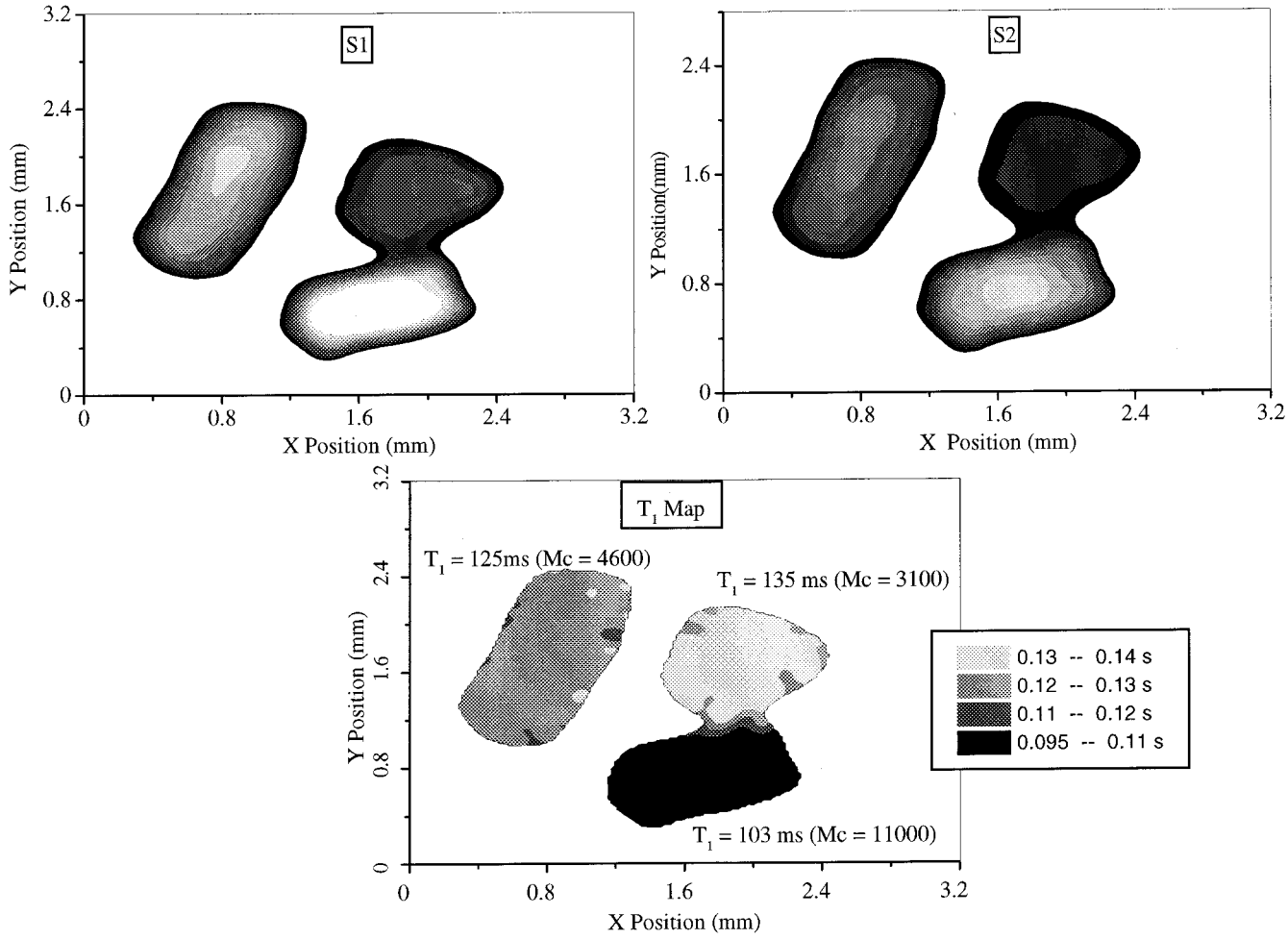

FIG. 3. Object consisting of three rubber samples of ca. 2 mm thickness. Experimental conditions are identical to those of Fig. 2 except for the parameters of the SUFIR sequence (τ = 169 ms, n = 512). Top: S_1 and S_2 (see Fig. 1) spin density images. Comparison pixel by pixel of these two images (according to Eq. [1]) yields the T_1 map (bottom). The T_1 value in the three samples is related to different molecular masses (M_c) of intercrosslink chains.

characteristic repetition time of the experiment ($0.5\ T_1 < \tau < 3\ T_1$) makes it sufficiently fast and, in any event, avoids the need to a complete return to thermal equilibrium.

The next step is to make this experiment space dependent. This can be accomplished fairly easily by means of radiofrequency field gradients (B_1 gradients) whose virtue is to perform simultaneously two actions: spatial labeling and spin excitation. Suppose that each normal fid acquisition in the SUFIR sequence is replaced by a train of short B_1 gradient pulses with acquisition of a single data point between two consecutive pulses. As reported before (*15, 16*), the Fourier transform of the pseudo-fid so obtained yields a profile representative of the projection upon the *spatial* axis along which the B_1 gradient is applied. Comparing the two results corresponding to S_1 and S_2 provides the relaxation time at each point of the profile. A 2D map can subsequently be produced with the help of an imaging experiment previously published (*17*). Let us recall that, as the gradient is available only in one direction, this experiment involves sample rotation step by step and a data treatment based on the projection reconstruction principle along with an adaptation of the "Filtered Back Projection" algorithm. Analysis pixel by pixel according to Eq. [1] leads to the required T_1 map. Of course, this implies that a single T_1 value is associated with each pixel.

The first test was carried out with a phantom made of two capillaries containing water with different amounts of copper sulfate so that the corresponding longitudinal relaxation times are 365 and 200 ms, respectively. These two capillaries are properly positioned by means of a Teflon holder. As shown in Fig. 2, the results are especially clean with an accuracy of $\pm 3\%$. It can be noticed that the capillary limits exhibit a clear-cut character which obviously does not exist in simple spin density images. This is due to the property that each pixel is associated with a unique T_1 value.

The second example (Fig. 3) is more directed to possible applications. The three rubber samples differ by their proton longitudinal relaxation times ranging from 100 to 135 ms. The corresponding spin density images exhibit nonuniformities due to the sample irregular thickness whereas a clear discrimination appears in the T_1 map. The border between the two nearby samples (bottom right) is actually visualized, demonstrating the resolution enhancement with respect to spin density images. Moreover, the differentiation between rather close T_1 values as well as their accuracy is definitely established.

In conclusion, we have proposed a very simple experiment yielding accurate T_1 images with enhanced spatial resolution and in a measuring time roughly twice that required for a conventional spin density image. Moreover, it can be noticed that such an efficiency stems from a unique property of B_1 gradients, that is the concomitant capability of spin excitation and spatial labeling.

REFERENCES

1. W. S. Price, NMR imaging, *Ann. Rep. NMR Spectrosc.* **35,** 139–216 (1998).
2. P. A. Gowland, M. O. Leach, and J. C. Sharp, The use of an improved inversion pulse with the spin–echo/inversion-recovery sequence to give increased accuracy and reduced imaging time for T_1, *Magn. Reson. Med.* **12,** 261–267 (1989).
3. J. J. Attard, S. J. Doran, N. J. Herrod, T. A. Carpenter, and L. D. Hall, Quantitative NMR spin-lattice relaxation imaging of brine in sandstone reservoirs cores, *J. Magn. Reson.* **96,** 514–525 (1992).
4. S. J. Doran, J. J. Attard, T. P. L. Roberts, T. A. Carpenter, and L. D. Hall, Consideration of random errors in the quantitative imaging of NMR relaxation, *J. Magn. Reson.* **100,** 101–102 (1992).
5. S. J. Doran, T. A. Carpenter, and L. D. Hall, Non invasive measurements of temperature distributions with high spatial resolution using quantitative imaging of NMR relaxation times, *Rev. Sci. Instrum.* **65,** 2231–2237 (1994).
6. G. F. Mason, W.-J. Chu, and H. P. Hetherington, A general approach to error estimation and optimized experiment design, applied to multislice imaging of T_1 in human brain at 4.1. T, *J. Magn. Reson.* **126,** 18–29 (1997).
7. A. Jivan, M. A. Horsfield, A. R. Moody, and G. R. Cherryman, Dynamic T_1 measurement using snapshot-FLASH MRI, *J. Magn. Reson.* **127,** 65–72 (1997).
8. I. Kay and R. M. Henkelmann, Practical implementation and optimization of T_1 imaging, *Magn. Reson. Med.* **22,** 414–424 (1991).
9. Y. T. Zhang, H. N. Yeung, P. L. Carson, and J. H. Ellis, Experimental analysis of T_1 imaging with a single scan, multiple-joint, inversion-recovery, *Magn. Reson. Med.* **25,** 337–343 (1992).
10. P. Gowland and M. O. Leach, Fast and accurate measurements of T_1 using a multi-readant single inversion-recovery sequence, *Magn. Reson. Med.* **26,** 79–88 (1992).
11. D. C. Look and D. R. Locker, Time saving in measurement of NMR and EPR relaxation times, *Rev. Sci. Instrum.* **41,** 250–251 (1970).
12. D. Canet, J. Brondeau, and K. Elbayed, Superfast T_1 determination by Inversion-Recovery, *J. Magn. Reson.* **77,** 483–490 (1988).
13. D. Canet, G. C. Levy, and I. R. Peat, Time saving in ^{13}C spin-lattice relaxation measurements by inversion-recovery, *J. Magn. Reson.* **18,** 199–204 (1975).
14. D. Canet, P. Mutzenhardt, and J.-B. Robert, The superfast inversion-recovery (SUFIR) experiment, *in* "Methods for Structure Elucidation by High-Resolution NMR" (Gy. Battá, K. E. Köver, and Cs. Szantay, Jr., Eds.), pp. 317–324. Elsevier, Amsterdam, 1997.
15. D. Boudot, D. Canet, and J. Brondeau, Spatial labeling by radiofrequency field gradient. DANTE-Z profile, probed by one-dimensional nutation imaging, *J. Magn. Reson.* **87,** 385–394 (1990).
16. D. Canet, Radiofrequency field gradient experiments, *Progr. NMR Spectrosc.* **30,** 101–135 (1997).
17. P. Maffei, P. Mutzenhardt, A. Retournard, B. Diter, R. Raulet, J. Brondeau, and D. Canet, NMR Microscopy by radiofrequency field gradients, *J. Magn. Reson. A* **107,** 40–49 (1994).
18. F. Humbert, B. Diter, and D. Canet, NMR microscopy by strong radiofrequency field gradients with spatial resolution better than five micrometers, *J. Magn. Reson. A* **123,** 242–245 (1996).